

A STUDY OF MORPHOLOGICAL, THERMAL, MECHANICAL AND BARRIER PROPERTIES OF PLA BASED BIOCOMPOSITES PREPARED WITH MICRO AND NANO SIZED CELLULOSIC FIBERS

ALI ABDULKHANI,^{*} JABER HOSSEINZADEH,^{*} SAEED DADASHI^{**} and MOHAMMAD MOUSAVI^{**}

^{*}*Department of Wood and Paper Science and Technology, Faculty of Natural Resources, University of Tehran, Karaj, Iran*

^{**}*Department of Food Science and Technology, Faculty of Agriculture Engineering and Technology, University of Tehran, Karaj, Iran*

✉ *Corresponding author: Ali Abdolkhani, Abdolkhani@ut.ac.ir*

Polylactic acid (PLA) nanocomposites with embedded acetylated cellulose nanofiber (CNF-Ac) and microcrystalline cellulose (MCC) were prepared using a solvent casting procedure. The microstructure, topography, barrier, mechanical and thermal properties of the composites were evaluated. Scanning electron microscopy micrographs clearly reveal uniform distribution of the reinforcing particles in the polymer at low loading levels (1 and 3 wt%), while higher content (5 wt%) of CNF-Ac and MCC contributed to easy aggregation within the matrix. The mechanical properties of the CNF-Ac incorporated composites were substantially increased in comparison with MCC filled PLA films. Comparing with nanocomposites, water vapor permeability of the MCC composites was increased at low content of MCC in the films. The tensile strength and tensile modulus of the composites with different loadings of MCC and 1 wt% CNF-Ac did not show any significant change. However, the strain of nano and micro filled composites was increased by more than 60% and 35%, respectively. The tensile strength, tensile modulus and strain were significantly increased for nanocomposites with 3 and 5 wt% CNF-Ac. Glass transition temperature of PLA was increased as a result of the incorporation with nanocellulose, while it was decreased by the incorporation of the films with microcrystalline cellulose.

Keywords: cellulose, polylactic acid, nanofiber, microcrystalline cellulose, nanocomposite

INTRODUCTION

Global environmental concerns create the necessity to replace petroleum-based materials by sustainable renewable resources to reduce the negative ecological effect of polymeric materials. In this context, bio-based polymers, i.e. polymers produced from renewable feedstock, might replace oil-based sources due to their numerous ecological benefits.¹ Different sources of naturally derived materials have been extensively used to produce green products.² During the last two decades, substantial progress has been made to produce biodegradable composites.³ Thermoplastic polymers were compounded with biomaterials to reduce production costs, while maintaining original properties.⁴ The development of environmentally friendly plastics for production of composites and nanocomposites is ultimately promising.^{3,5} Aliphatic biodegradable

polyesters, such as polylactic acid (PLA), polycaprolactone (PCL), poly(3-hydroxybutyrate) (PHB), and polyglycolic acid (PGA), have been widely compounded with different materials to produce green composites.⁶ PLA is one of the most promising alternatives to typical plastics and has gained much attention mainly due to its biodegradability.^{7,8} However, the poor thermal and mechanical resistance and limited gas barrier properties compared to petroleum-based polymers are the main limitations of widespread application of PLA in packaging industries.^{9,10} The processing issues of PLA have been addressed by enhancing their thermomechanical properties through copolymerization, blending and filling techniques. Cellulose, the most abundant biopolymer, has been found to possess attractive mechanical properties that make possible its use

as reinforcing material in combination with PLA polymer composites.¹¹ Fiber reinforced composites have received much attention mainly due to their low density, low price, as well as nonabrasive, nontoxic, and biodegradable properties. Many studies have been carried out to investigate the reinforcing ability of cellulosic fibers in different composites.¹²⁻¹⁶ PLA was reinforced with nanocellulose by solvent casting and melt compounding procedures.¹⁷⁻¹⁹ Microcrystalline cellulose (MCC) was used in several studies to enhance the mechanical properties of PLA nanocomposites.¹⁹⁻²²

Comprehensive and comparative studies have been reported on the isolation and characterization of micro to nanoscale cellulosic fibers from kenaf bast.^{23,24,25} The production of microfibrillated cellulose (MFC)-reinforced polylactic acid (PLA) nanocomposites from sheets obtained by a papermaking-like process has been studied.²⁴ Also, cellulose nanofibers isolated by acid treatment of commercial microcrystalline cellulose were used to prepare composites with polylactic acid by melt compounding.²⁵ A systematic comparison between the reinforcing effects of micro and nano cellulosic particles has not been reported so far on polylactic acid based composites. The present study aims to evaluate the different functional properties of PLA films reinforced with microcrystalline cellulose (MCC) and acetylated cellulose nanofiber (CNF-Ac). The effect of micro and nanoscale cellulose loadings on the phase morphology, topography, physical, mechanical, thermal and barrier properties of PLA composite films was investigated.

EXPERIMENTAL

Materials

Poly(lactic acid) (Bio-flex®F 6510) was provided from Fkur Kunststoff GmbH (Siemensring 79, Germany) with a density of 1300 kg/m³, melting point of 150-170 °C and molecular weight (M_w) of 197000 g/mol. PLA resins were dried in a vacuum oven at 60 °C for 24 hours before casting. All the necessary chemicals were provided from Merck (Merck, Darmstadt, Germany) and were used as received. Acetylated cellulose nanofiber (CNF-Ac) gel (3 wt%) was provided from Novin Polymer Co. (Tehran, Iran). Microcrystalline cellulose (MCC) was obtained from Asahi Kasei Chemicals Corp. (Tokyo, Japan).

Modification of cellulose

A solution mixture of acetic acid (25%) and sulfuric acid (3%) was used to activate CNF at 70 °C

for 30 min. The acetylation of CNF was performed by adding 10 mL anhydride acetic and 50 mL acetic acid. The mixture was stirred for 4 h at 100 °C. The acetylated CNF was then added to a solution of acetone: methanol (2:1, v:v) and subsequently chloroform to fulfill the sequential phase transition of acetylated fibers to chloroform.

Film preparation

PLA and PLA composite films were prepared using a solvent casting process, according to the method described by Rhim *et al.*²⁶ with small modifications. PLA (5 g) was dissolved in chloroform (100 mL) and vigorously agitated for 8 h at room temperature (25 °C). The solution was then poured into greased glass molds, followed by drying at room temperature for 24 h. For the preparation of PLA nanocomposite films, a preweighed amount of CNF-Ac (0.05, 0.15 and 0.25 g) and MCC were suspended in chloroform under vigorous stirring for 8 h using a magnetic stirrer. The mixed materials were then homogenized at 8000 rpm for 15 min in an ultra-turrax T-25 homogenizer (IKA T25-digital ultra turrax, Staufen, Germany) with a S25N-25F probe, followed by sonication for 30 min at room temperature by a high intensity ultrasonic processor (Model VCX 750, Sonics & Materials Inc., Newtown, CT, USA). Solutions containing 1, 3 and 5 wt% CNF and MCC were added to the previously prepared PLA solution and then stirred vigorously for 15 min with a magnetic stirrer. The solutions were homogenized at 8000 rpm for 15 min and sonicated for another 30 minutes, and then put into greased glass molds. The final film was obtained by the procedure explained above for pure PLA films. After drying at room temperature for 24 h, all PLA/composite films were further dried at 60 °C in a vacuum dryer to get rid of the remaining solvent.²⁷

Microstructure

The microstructure of both CNF-Ac and MCC fabricated composite films was analyzed by scanning electron microscopy (SEM) (Philips-XL30, Rotterdam, Netherlands). Specimens were prepared using standard techniques, mounted on aluminum stubs, and sputter coated with gold (100 Å).²⁸ The micrographs were collected using an accelerating voltage of 25-30 kV. The topography of the films that had been previously equilibrated at a relative humidity of 50% was studied using an atomic force microscope (AFM) (Q-Scope 250, Quesant, California, USA). Samples were cut into thin pieces to fit into AFM imaging, and were stuck onto the sample stage. Contact cantilever with broadband scan mode was used to record the micrographs. The resulting data for each sample were transformed into a 3D image.²⁷ To make the results comparable, the images were chosen from the central area of each surface.

Mechanical properties

A Testometric Machine M350-10CT (Testometric Co. Ltd., Rochdale, Lancs., England) was used to study tensile strength and tensile modulus of the specimen according to ASTM standard method (ASTM, D882-91, 1996). The initial grip separation and crosshead velocity were set to 50 mm and 50 mm/min, respectively. Tensile strength was calculated by dividing the maximum load on the film before failure by the cross-sectional area of the initial specimen. Tensile modulus was determined according to the slope of the stress/strain curve in the linear range. Strain was defined as the percentage change in the length of the specimen to the original length between the grips. At least five replicates were obtained for each sample.

Thermal properties

Glass transition temperature and melting point temperature of the PLA-based composite films prepared by the solvent casting method were studied by DSC (DSC Pyris 6, Perkin Elmer Co. USA). 2-4 mg specimens were sealed in standard aluminum pans using a sealed empty aluminum pan as reference. Experiments were conducted in the range of -10 to 200 °C with a heating rate of 10 °C/min. The degree of crystallinity ($\chi\%$) was calculated using a value of 93 J/g for the heat of fusion of the 100% crystalline PLA.²⁹

Water vapor permeability

Water vapor permeability was gravimetrically measured according to the standard method E96 (ASTM Standards, 1995) and similar to that adopted by Ghasemlou *et al.*³⁰ It was corrected for the stagnant air gap inside the test cups according to the equations of Gennadios *et al.*³¹ Special glass cups with wide rims were used to determine WVP. Anhydrous calcium chloride (80 g) was used for the purpose of permeability measurement. Briefly, films without pinholes or defects were cut circularly (with an area of 0.002827 m²) and sealed to the cup mouths using molten paraffin. Each cup was placed in a desiccator and maintained at 75% RH with a sodium-chloride-saturated solution. This difference in RH corresponds

to a driving force of 1753.55 Pa, expressed as water vapor partial pressure. After mounting the specimens, the weight gain of the whole assembly was recorded every 1 h during the first 9 h and finally, after 24 h (with an accuracy of 0.0001 g). The cups were shaken horizontally after every weighing. The slope of weight versus time plot (the lines' regression coefficients were >0.998) was divided by the effective film specimen area to obtain the water vapor transmission rate. This was multiplied by the thickness of the film and divided by the pressure difference between the inside and outside surfaces to obtain the water vapor permeability (Eq. 1).

$$WVP = \frac{\Delta m \cdot X}{A \Delta t \Delta P} \quad (1)$$

where $\Delta m/\Delta t$ is the weight of moisture gain per unit of time (g.s⁻¹), X is the average film thickness (m), A is the area of the exposed film surface (m²), and ΔP is the water vapor pressure difference between the two sides of the film (Pa). Water vapor permeability was measured in three replicates for each type of film.

RESULTS AND DISCUSSION

Microstructure

A SEM micrograph of acetylated CNF is presented in Figure 1. The diameter of nanofibers ranged between 5-80 nm with the average value of 28 nm. Micrographs of cryo-fractured surfaces of the neat PLA film and its associated composites are illustrated in Figures 2 and 3. No substantial deviation was detected in the micrographs of PLA/CNF-Ac 1% and 3% with the neat PLA film. The rough surface of the PLA/CNF-Ac 5% sample is obviously different from that of the other specimens. An aggregation of nanocellulose is visible within a small portion of this sample (Figure 2D). According to micrographs, a good level of CNF-Ac dispersion occurred in the composites with 1 and 3% CNF-Ac loadings.

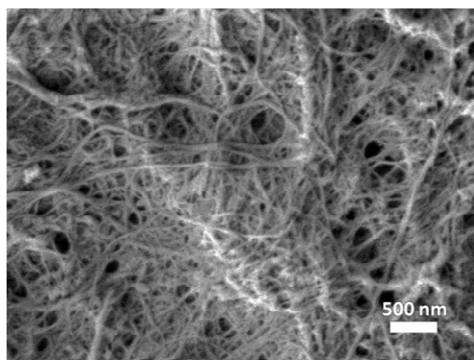


Figure 1: SEM image of CNF

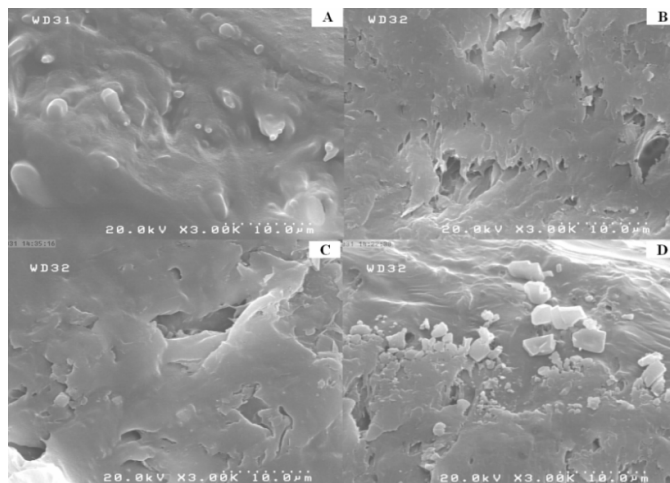


Figure 2: SEM images of cryo-fractured surfaces of A: neat PLA; B, C, D: PLA reinforced with 1, 3 and 5% CNF, respectively

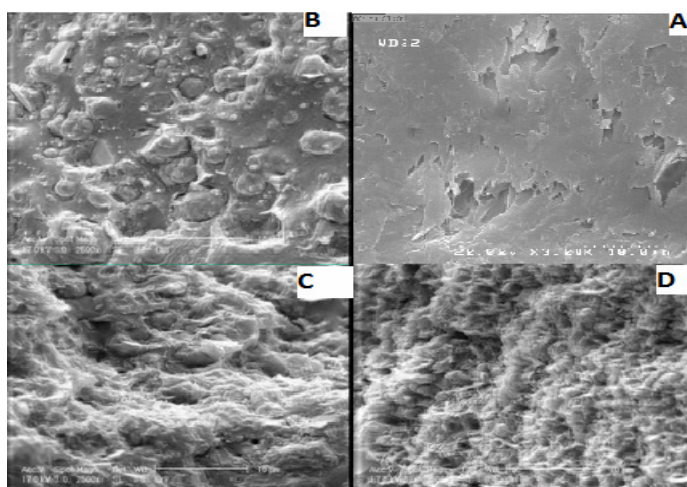


Figure 3: SEM micrographs of the cryo-fractured surfaces of A: neat PLA; B, C, D: PLA reinforced with 1, 3 and 5% MCC, respectively

The SEM micrograph of a cross section of the film with 1% MCC (Figure 3B) reveals uniform dispersion of the particles in comparison with higher MCC levels. According to Figures 3C and 3D, a compact sponge-like structure due to partial aggregation can be observed in the films with 3 and 5% MCC.

Surface topography of films by AFM

AFM has been broadly used to provide qualitative and quantitative information about biopolymers at the nanoscale.³² Figure 4 illustrates 3D topography images of the PLA-CNF and PLA-MCC films. According to Figure 4-A, the neat PLA has a relatively smooth and uniform surface. The surface roughness was

enhanced by the addition of 1, 3 and 5% acetylated cellulose nanofiber to the polymer.

The films fabricated with 1% CNF-Ac represent a uniform surface, which implies reasonable dispersion of nanofibers in the matrix, as well as good interfacial bonding between the phases. This is due to the low cellulose content, as well as to the increased compatibility of nanoparticles through the acetylation process.

A good dispersion of nanofibers in the gallery was observed for PLA reinforced with 3% CNF-Ac. Increasing the CNF-Ac loading to 5% caused a rough and non-uniform surface, implying poor dispersion of the CNF-Ac in the matrix. More investigations on the micrographs revealed that with an increment of nanofiber content, the thickness of the fabricated films increased

significantly. The results obtained from this topographical investigation can be very useful in designing various nanocomposite coatings and

especially the surface characteristics of various packaging materials.

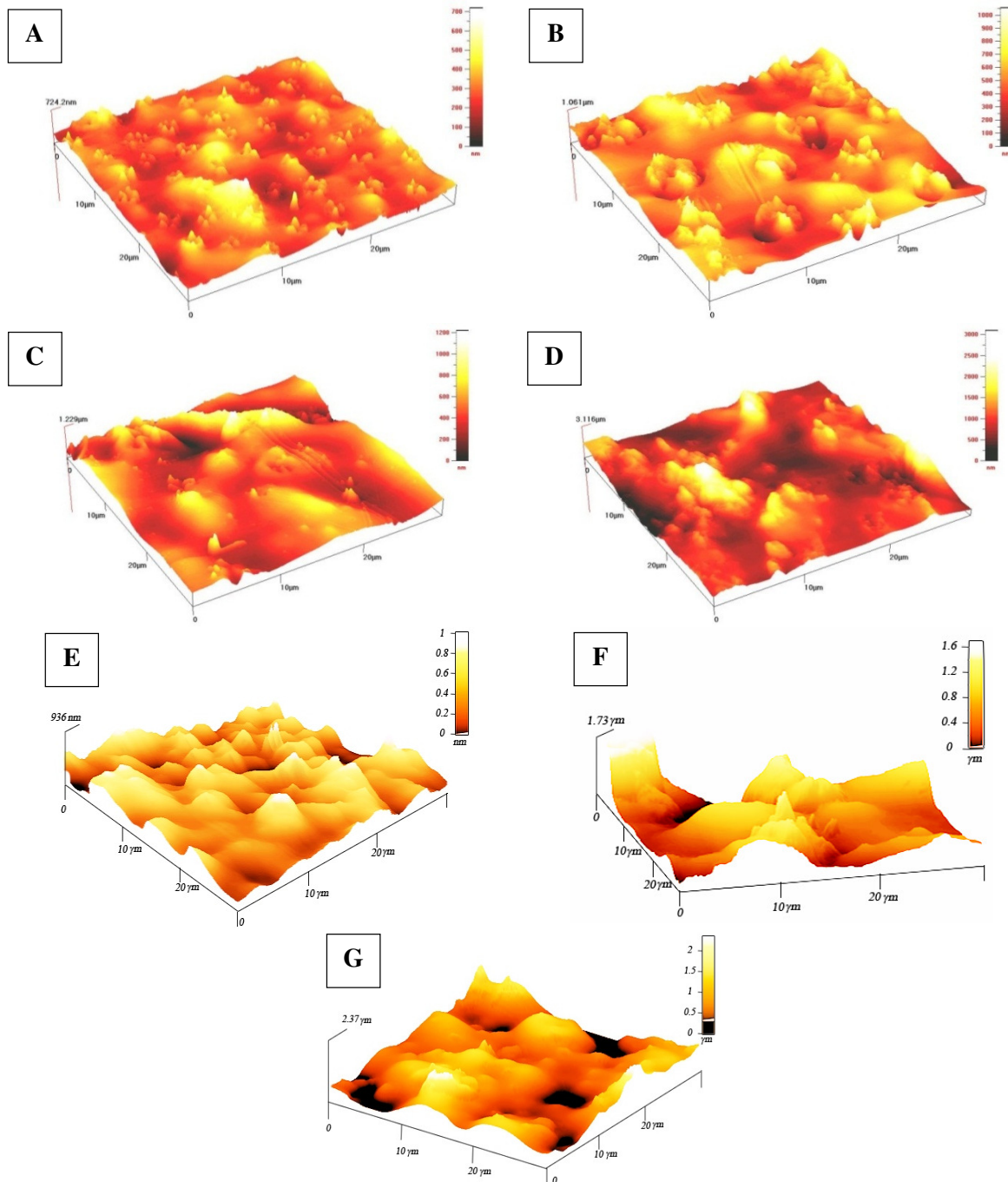


Figure 4: AFM topographic images of neat PLA (A), PLA/CNF-Ac-1 (B), PLA/CNF-Ac-3 (C), PLA/CNF-Ac-5 (D), PLA/MCC-1 (E), PLA/MCC-3 (F) and PLA/MCC-5 (G)

The surface roughness of the films was significantly increased by embedding MCC into

the polymer, due to its hydrophilicity and dimensions compared with acetylated CNFs.

Mechanical properties

The effects of the mechanical tests of PLA and its nanocomposite films, including tensile strength, tensile modulus and strain are depicted in Figure 5. Quantitative data are presented in Table 1. The tensile strength, tensile modulus and strain of neat PLA film were 15.24 MPa, 1.17 GPa and 40.30%, respectively. By incorporating 1% CNF-Ac into PLA films, tensile strength, tensile modulus did not show significant changes, while E increased by more than 60 percent. This trend was improved by increasing the CNF-Ac portion to 3%, in which the tensile strength, tensile modulus increased to 33.06 MPa and 188.86%, respectively. It seems that nanofiber orientation occurred effectively in the PLA matrix and therefore the TS curve had an increasing trend in two stages during the stretching of the composite films. The tensile modulus of the 5% films increased by 81% at the expense of a

significant decrease in the strain value by 64%. According to Dufresne *et al.*,³³ the overall mechanical performance of composites, particularly nanocomposites, depends on six factors: 1) adhesion and compatibility between the polymer matrix and additives, 2) stress transfer efficiency of additives, 3) volume fraction of additive, 4) aspect ratio of additive, 5) the orientation of additives and 6) crystallinity of the matrix. Iwatake *et al.*²¹ reported an improvement in the mechanical properties of PLA composites by the addition of acetylated cellulose nanofibers due to an increase in compatibility between the moieties. The dispersion of CNF-Ac within the PLA matrix was absolutely improved by using ultra turrax and ultrasonic treatments. However, fiber accumulation in the loading beyond 3% caused a drop in the mechanical properties of the fabricated film, as shown in Figure 5.

Table 1
Mechanical properties of PLA-cellulose nanocomposites

Composition	Tensile strength (MPa)	Tensile modulus (GPa)	Strain (%)
PLA	15.24±4.90b	1.17±0.38b	40.30±5.6c
PLA/CNF-Ac-1	16.70±3.76b	1.13±0.04b	64.77±4.72b
PLA/CNF-Ac-3	33.06±3.90a	1.20±0.41b	188.86±12.92a
PLA/CNF5-Ac-5	30.54±1.60a	2.12±0.27a	14.62±3.32c
PLA/MCC-1	15.66±4.14	1.25±0.24	35.91±2.68
PLA/MCC-3	15.88±2.83	1.19±0.20	38.47±1.96
PLA/MCC-5	16.52±2.26	1.18±0.18	39.95±3.34

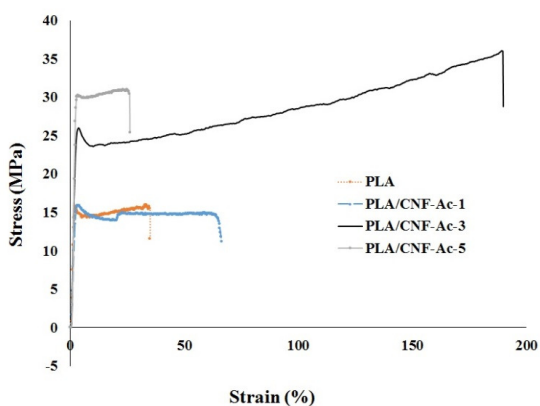


Figure 5: Stress-strain curves of pure PLA and its nanocomposites

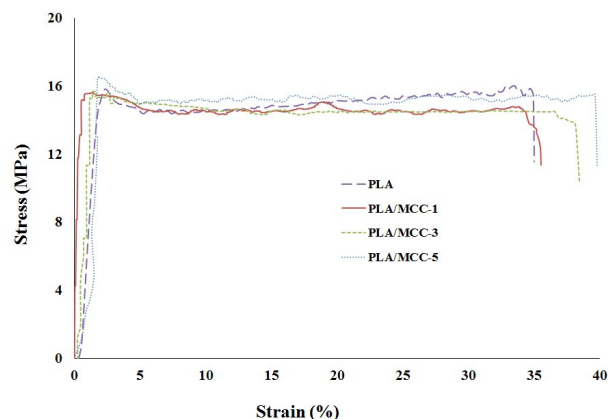


Figure 6: Stress-strain curves of pure PLA and its composites

Likewise, composition of the MCC with PLA in all loadings does not lead to significant gains in the mechanical strength of the fabricated PLA films (Figure 6 and Table 1). This is because of

the poor compatibility and interfacial interaction between MCCs and PLA matrix and the large size of the incorporated cellulosic fibers. A small increase of tensile strength was observed in

PLA/MCC-5. The Tensile strength and tensile modulus values of PLA/MCC-5 film were measured as 16.52 MPa and 1.18 GPa, respectively.

Thermal analysis (DSC)

DSC analysis was carried out in order to investigate the effect of acetylated CNFs and MCCs composition on the thermal properties of the PLA matrix. Glass transition temperature (T_g), cold crystallization temperature (T_c) and melting point (T_m) were recorded for the fabricated PLA films (Table 2). Glass transition temperature for CNF-Ac reinforced specimens was in the range of 57 to 59 °C. A minor improvement in T_g value was observed by incorporation of acetylated CNF into PLA (Table

2). Melting enthalpy was reduced from 34.23 J/gr for the neat PLA film to 33.86, 29.55 and 29.88 for 1, 3 and 5% CNF-Ac reinforced films, respectively. The calculated crystallinity (X_c) was decreased by the addition of acetylated CNFs, implying a change in the crystalline structure of the pure PLA matrix when semi-amorphous nanofibers were embedded in the matrix during the casting process. According to the DSC results, the melting point of different films was unchanged regardless of loading. The obtained results for MCC composites (Table 2) revealed a particular behavior of these nanoparticles. In the PLA films with 3% MCC, a substantial drop in T_g from 57.47 °C to 48.46 °C occurred. However, the glass transition temperature increased to 53.79 °C when increasing the MCC content to 5%.

Table 2
Thermal characteristics of the samples determined by DSC

Composition	T_g (°C)	T_m (°C)	ΔH_m (J/g)	X_c (%)
PLA	57.47	156.28	34.23	39.34
PLA/CNF-Ac-1	58.26	150.57	33.86	38.92
PLA/CNF-Ac-3	58.48	154.21	29.55	33.96
PLA/CNF-Ac-5	58.94	154.08	29.88	34.34
PLA/MCC-1	48.46	154.83	34.18	38.12
PLA/MCC-3	51.03	155.64	34.89	39.30
PLA/MCC-5	53.79	155.64	34.18	39.65

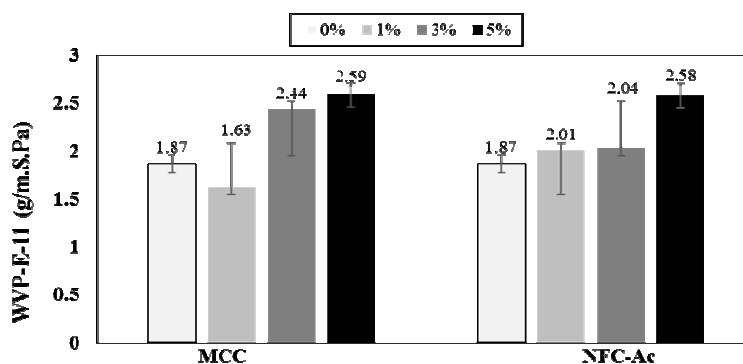


Figure 7: Effect of NFC-Ac content (wt%) on the WVP of PLA nanocomposites

According to the results of the X_c , the addition of MCC to the PLA does not lead to a significant change in crystallinity. The melting point temperature of MCC filled films decreased slightly, indicating a weak interaction between MCC and the polymeric substrate. Regarding T_g variations, it is worth noting that an increase or decrease of this parameter is not necessarily

aligned with the change in the crystallinity of the material. The mobility of polymeric chains is one of the important factors in T_g variation. Therefore, loading the PLA with MCC improved the regularity of its amorphous phase and consequently the T_g value of the fabricated PLA-MCC film.

Water vapor permeability

Since water is one of the most important causes of food spoilage reactions, water vapor permeability (WVP) is one of the most important features of food packaging materials. The results of WVP measurements of pure PLA, PLA reinforced with MCC and PLA reinforced with nanocellulose are illustrated in Figure 7. According to the results, a permeability value of 1.87×10^{-11} (g/m.S.Pa) was recorded for pure PLA, which is in agreement with the value reported by Auras *et al.*³⁴ Furthermore, with the addition of 1 and 3% CNF-Ac to the polymeric matrix, WVP was increased to the values of 2.01×10^{-11} and 2.04×10^{-11} , respectively. These results indicate that 1 and 3% acetylated nanocellulose have uniform distribution and good compatibility with the polymeric matrix and could effectively fill up the polymer pores. A significant increase in WVP (38.5%) was observed for the CNF-Ac 5% film. Obviously, the WVP decreased to some extent by the addition of 1% MCC to the matrix. This value was increased by 30.48% and 38.50% when the proportion of MCC was increased to 3 and 5%, respectively.

MCC is a hydrophilic polysaccharide; therefore, its application as reinforcing agent in polymeric matrices should be restricted to the amount that does not affect the texture of the polymer. Uniform distribution of particles within the polymer could be an explanation for reducing the WVP in the case of the 1% MCC film. However, reinforcing the composite with 3 and 5% hydrophilic MCC led to an increase in WVP.³⁵

CONCLUSION

Poly(lactic acid) based biocomposites reinforced with nano and micro cellulosic fibers were prepared by a solution casting method to investigate the effect of fiber dimension on green composite properties. Morphological and topographical analysis of the composite films with SEM and AFM indicated the appropriate dispersion of the nanocellulosic fibers within the matrix at 1 and 3% loadings and subsequent improvement in strength properties. Increasing the nanofiber loading to 5%, however, led to an aggregation of fibers. The tensile strength of the MCC reinforced composite decreased due to the inappropriate dispersion of the particles within the matrix. The glass transition temperature (T_g) of the composites decreased from 57.47 to 46.48 °C in the 1% MCC filled composite. WVP results

showed that the addition of CNF-Ac at 1 and 3% had no significant effect on the water vapor permeability, while loading the matrix with MCC led to a significant increase in vapor transmission.

REFERENCES

- ¹ D. Klemm, D. Schumann, F. Kramer, N. Heßler, M. Hornung *et al.*, *Adv. Polym. Sci.*, **205**, 49 (2006).
- ² H. X. Fang, J. Y. Sun and L. Zhang, *Polym. Mater. Sci. Eng.*, **25**, 148 (2009).
- ³ H. Yousefi, T. Nishino, M. Faezipour, G. Ebrahimi and A. Shakeri, *Biomacromolecules*, **12**, 4080 (2011).
- ⁴ M. Kowalczyk, E. Piorkowska, P. Kulpinski and M. Pracella, *Compos. Part A: Appl. S.*, **42**, 1509 (2011).
- ⁵ M. J. John and S. Thomas, *Carbohydr. Polym.*, **71**, 343 (2008).
- ⁶ N. Guigo, L. Vincent, A. Mija, H. Naegelé, N. Sbirrazzuoli, *Combust. Sci. Technol.*, **69**, 1979 (2009).
- ⁷ O. Avinc and A. Khoddami, *Fibre Chem.*, **41**, 391 (2009).
- ⁸ A. Gupta and A. Kumar, *Asian J. Chem.*, **24**, 1831 (2012).
- ⁹ B. Singh, M. Gupta, A. Verma, *Compos. Part A: Appl. S.*, **34**, 1035 (2003).
- ¹⁰ R. P. Singh, J. K. Pandey, D. Rutot, P. Degée and P. Dubois, *Carbohydr. Res.*, **338**, 1759 (2003).
- ¹¹ A. Iwatake, M. Nogi and H. Yano, *Combust. Sci. Technol.*, **68**, 2103 (2008).
- ¹² S. Kalia, B. S. Kaith and I. Kaur, *Polym. Eng. Sci.*, **49**, 1253 (2009).
- ¹³ W. G. Glasser, R. H. Atalla, J. Blackwell, R. M. Brown Jr, W. Burchard *et al.*, *Cellulose*, **19**, 589 (2012).
- ¹⁴ N. Sgriccia, M. C. Hawley and M. Misra, *Compos. Part A: Appl. S.*, **39**, 1632 (2008).
- ¹⁵ M. Mariano, N. El Kissi and A. Dufresne, *J. Polym. Sci., Part B: Polym. Phys.*, **52**, 791 (2014).
- ¹⁶ S. Karimi, P. Md. Tahir, A. Dufresne, A. Karimi and A. Abdulkhali, *Nord. Pulp Pap. Res. J.*, **29**, 41 (2014).
- ¹⁷ C. Chang, I. C. Wang, Y. S. Perng, *Cellulose Chem. Technol.*, **47**, 111 (2013).
- ¹⁸ D. Bondeson and K. Oksman, *Compos. Interfaces*, **14**, 617 (2007).
- ¹⁹ K. Oksman, A. P. Mathew, D. Bondeson and I. Kvien, *Combust. Sci. Technol.*, **66**, 2776 (2006).
- ²⁰ N. Bitinis, R. Verdejo, J. Bras, E. Fortunati, J. M. Kenny *et al.*, *Carbohydr. Polym.*, **96**, 611 (2013).
- ²¹ M. K. M. Haafiz, A. Hassan, Z. Zakaria, I. M. Inuwa, M. S. Islam *et al.*, *Carbohydr. Polym.*, **98**, 139 (2013).
- ²² A. P. Mathew, K. Oksman and M. Sain, *J. Appl. Polym. Sci.*, **101**, 300 (2006).
- ²³ S. Karimi, P. M. Tahir, A. Karimi, A. Dufresne and A. Abdulkhali, *Carbohydr. Polym.*, **101**, 878 (2014).
- ²⁴ A. N. Nakagaito, A. Fujimura, T. Sakai, Y. Hama and H. Yano, *Combust. Sci. Technol.*, **69**, 1293 (2009).
- ²⁵ A. N. Frone, S. Berlioz, J. F. Chailan and D. M. Panaitescu, *Carbohydr. Polym.*, **91**, 377 (2013).

- ²⁶ J. W. Rhim, S. I. Hong and C. S. Ha, *J. Food Sci. Technol.*, **42**, 612 (2009).
- ²⁷ J. W. Rhim, A. K. Mohanty, S. P. Singh and P. K. W. Ng, *J. Appl. Polym. Sci.*, **101**, 3736 (2006).
- ²⁸ M. E. Gounga, S. Y. Xu and Z. Wang, *J. Food Eng.*, **83**, 521 (2007).
- ²⁹ E. W. Fischer, H. J. Sterzel and G. Wegner, *Colloid. Polym. Sci.*, **251**, 980 (1973).
- ³⁰ M. Ghasemlou, F. Khodaiyan and A. Oromiehie, *Carbohydr. Polym.*, **84**, 477 (2011).
- ³¹ A. Gennadios, C. L. Weller and C. H. Gooding, *J. Food Eng.*, **21**, 395 (1994).
- ³² B. Ghanbarzadeh, M. Musavi, A. R. Oromiehie, K. Rezayi, E. Razmi Rad *et al.*, *J. Food Sci. Technol.*, **40**, 1191 (2007).
- ³³ A. Dufresne, D. Dupeyre and M. Paillet, *J. Appl. Polym. Sci.*, **87**, 1302 (2002).
- ³⁴ R. Auras, B. Harte and S. Selke, *J. Appl. Polym. Sci.*, **92**, 1790 (2003).
- ³⁵ L. Petersson and K. Oksman, *Compos. Sci. Technol.*, **66**, 2187 (2006).